

HIGH-ENERGY MUON GENERATION IN COSMIC RAYS

T.P. Amineva, I.P. Ivanenko, M.A. Ivanova, K.V. Mandritskaya, E.A. Murzina, S.I. Nikolsky~~*,~~, E.A. Osipova, I.V. Rakobolskaya, N.V. Sokolskaya, N.I. Tulinova, A.Ya. Varkovitskaya, E.A. Zamchalova, G.T. Zatsepin ~~***~~.

Institute of Nuclear Physics of Moscow State University, Lebedev Physical Institute of the Academy of Sciences of the USSR~~*,~~, Institute of Nuclear Research of the Academy of Sciences of the USSR. ~~***~~

State University, Moscow 117234, USSR.

An X-ray-emulsion chamber installation for detection of bremsstrahlung photons produced by muons in lead has made it possible to obtain: (1) zenith angular distribution of ≥ 2 TeV muons. The obtained distribution agrees with calculations made on the assumption that the muons are produced in the decays of pions or pions mixed with 20% of kaons; (2) the (2-20) TeV muon energy spectra within the entire range of zenith angles. Up to ~ 8 TeV the spectra agree with the assumption that the muons are generated in the decays of pions and kaons displaying a power form of their spectrum with the same exponent as the primary nucleon spectrum.

1. Introduction. An increased interest to the cosmic ray muon studies arose from works by Bergeson et al. (1967, 1971) where a more isotropic angular distribution of high-energy muons was obtained than expected from the idea of muon production in the processes of π and K decay (Alekseev and Zatsepin, 1959). The muon energy spectrum with exponent $\gamma = 2.0 \div 2.2$ obtained in (Christiansen et al., 1971; Erlykin et al., 1971) was also at variance with this idea. It was important, therefore, to simultaneously measure the muon energy spectrum and angular distribution with a single installation.

2. The installation. The use was made of 130 X-ray-emulsion chambers detecting the bremsstrahlung photons produced by muons in lead (Amineva et al., 1971; 1972). The number of photons produced in other processes of the muon interaction with matter is small due to great Z^2/A of lead, and therefore, it is possible to safely turn from the spectrum and angular distribution of electron-photon cascades (EPC) to the same distributions for muons. The chambers were so arranged in an underground room that the X-ray film planes were at 45° and 60° to the horizontal plane. This permitted both vertical and horizontal muon fluxes to be measured.

Such installation is advantageous because of its high transmission determined by the lead mass, exposure time, and installation geometry: $M \cdot T \cdot 2\pi K$

Presented in this report are the data obtained at an exposure of 380 ton. year which is equivalent to $\sim 7 \cdot 10^{10} \text{ cm}^2 \cdot \text{sec. ster.}$ if the EPC detection effectiveness, installation solid angle, and probability of a bremsstrahlung photon production by a muon are included.

The installation effectiveness, K , was calculated using the Monte-Carlo method at the various limitations imposed on angle ψ between EPC and film, EPC energy - E_0 , and zenith angle Θ .

The calculations have shown that at $\psi \leq 60^\circ$ the value of K is independent of EPC energies from $E_0 = 2.0 \text{ Tev}$ (effectiveness for $E_0 = 1.6 \text{ rev}$ is 10% lower) and is energy-independent for the cascades with $E_0 \geq 3.2 \text{ Tev}$ up to the values of $\psi = 72^\circ$. For the total muon flux throughout the Θ range the values of the effectiveness at $\psi \leq 60^\circ$ are: $K_{45^\circ} = 0.36$ and $K_{60^\circ} = 0.38$, whereas at $\psi \leq 72^\circ$ $K_{45^\circ} = 0.51$ and $K_{60^\circ} = 0.53$.

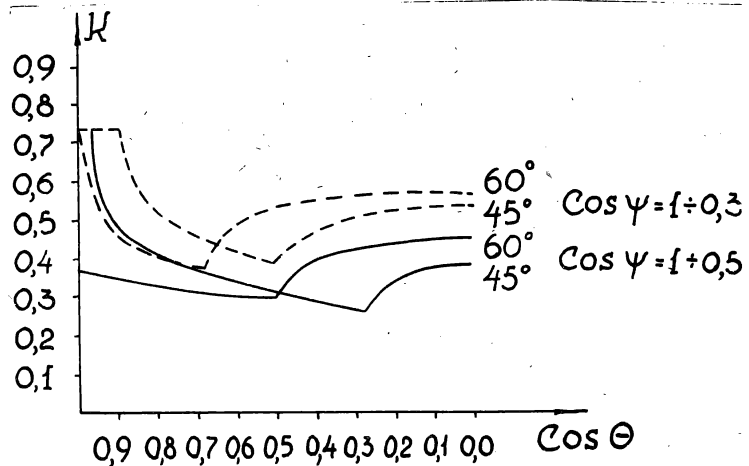


Fig. 1. The $E \geq 2 \text{ Tev}$ EPC detection effectiveness shown as a function of $\cos \Theta$

Only the cascades for which $\psi \leq 60^\circ$ were used when plotting the muon energy spectra and zenith angular distribution in the 2.0 - 4.0 Tev EPC energy range, and it was not until 4.0 Tev when all the events at $\psi \leq 72^\circ$ were included.

3. Experimental technique. The zenith angle Θ was found from the relation $\cos \mathcal{L} \cdot \cos \psi - \sin \mathcal{L} \cdot \sin \psi \cdot \sin \varphi = \cos \Theta$

where \mathcal{L} is the chamber inclination angle, φ is the azimuthal angle in the chamber plane. Given in Table 1 as a function of \mathcal{L} and ψ .

Table 1.

| $\mathcal{L} \backslash \psi$ | 1-0,9 | 0,9-0,8 | 0,8-0,7 | 0,7-0,6 | 0,6-0,5 | 0,5-0,4 | 0,4-0,3 | 0,3-0,2 | 0,2-0,1 | 0,1-0,0 |
|-------------------------------|-------|---------|---------|---------|---------|---------|---------|---------|---------|---------|
| 45° | 0,016 | 0,029 | 0,034 | 0,041 | 0,048 | 0,052 | 0,053 | 0,052 | 0,048 | 0,047 |
| 60° | 0,017 | 0,031 | 0,040 | 0,045 | 0,044 | 0,046 | 0,052 | 0,055 | 0,056 | 0,056 |

tion of $\cos \Theta$ are the mean errors in determination of $\cos \Theta$ due to inaccuracy of measurements of ψ , ψ and α for the various types of chambers.

The method for determining the EPC energies in an X-ray-emulsion chamber is based on the use of the core approximation in the EPC theory (Nishimura, 1964) and the calibration of blackening which relates the density of a black spot formed by an EPC in X-ray film to the electron flux density in the same cascade as seen in nuclear emulsion (Baradzei et al, 1971).

The energy of a single EPC was determined by plotting the curves relating the value of spot blackening in a single emulsion layer within circles of definite radius $D(R, E_0, \psi, t)$ to the cascade development depth for various values of E_0 and ψ . The cascade energy was determined on the basis of the curve describing best the experimental distribution.

The calculation curves were compared to the averaged experimental functions $\bar{D}(t)$. With this purpose the events which produced at least three black spots were selected and broked into several intervals for energies and angle ψ . Fig. 2 presents the calculation curves for two values of E_0 and ψ and the plots of the experimental mean values of $\bar{D}(t)$. They are in agreement within experimental errors.

Agreement between the forms of the experimental and calculated cascades is qualitatively characterized by the value

$$\chi^2 = \sum_{l=1}^n \frac{(D_{exp} - D_{calc})^2}{\sigma^2}$$

where σ is the error in measurements of blackening, and summation is made over all points of a single cascade. Analysis of the distribution of these values for all many-point cascades (more than 4 points) has shown that the number of the cases with high values of χ^2 is only 7% greater than that expected from statistical distribution. This fact is indicative of a good agreement between the forms of the experimental cascade and the cascade expected in terms of the electromagnetic theory. The cascade with high values of χ^2 may appear due to both methodical and physical causes. Possible roughness of lead and film defects should be considered as the methodical

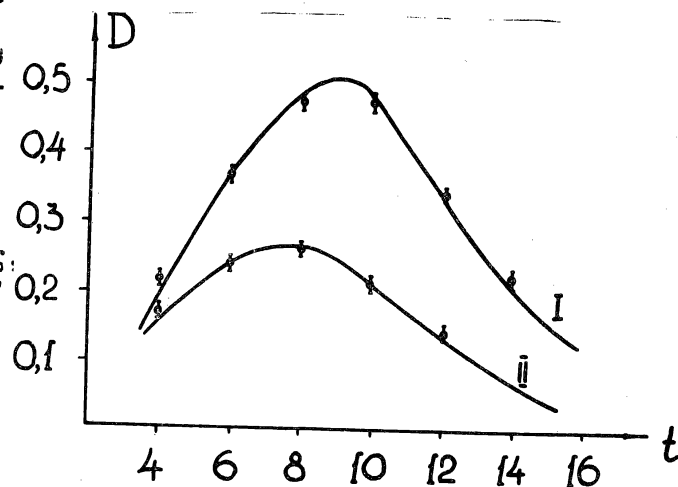


Fig.2. Comparison between the calculated cascade curves and mean distributions $\bar{D}(t)$
I. $E_0 = 4.7 \text{ Tev}$ II. $E_0 = 1.93 \text{ Tev}$ $\cos \psi = 0.9$

causes, while the physical causes may be the muon nuclear interactions or strong electromagnetic fluctuations in the particle number.

The method for determining the energy in the multilayer X-ray-emulsion chamber was absolutely calibrated at mountain level (700 g/cm²) using γ -quanta produced as a result of π^0 -meson decays in a target above the installation (Amineva et al., 1973). Analysis of the results obtained makes it possible to assert that in the 1.6 - 5 Tev EPC energy range the systematic error in energy determination does not exceed 7%.

Examination of possible methodical factors distorting the determined value of E_0 and role of the particle number fluctuations has shown that in a single case the EPC energy can be found in the multilayer X-ray-emulsion chamber within 20%. In this case the error is somewhat smaller for the many-point events. The error in the value of γ -quantum generation intensity is somewhat higher than the statistical one because of methodical effects and, according to our estimate, is 20-30%.

4. Experimental data. Table 2 lists the experimental data obtained with 130 chambers in several zenith angle ranges.

Table 2.

| E_{γ} rev | \bar{E}_{γ} | $1 \geq \cos \Theta > 0,6$ | | $0,6 \geq \cos \Theta > 0,3$ | | $0,3 \geq \cos \Theta \geq 0,0$ | | $1,0 \geq \cos \Theta \geq 0,0$ | |
|------------------|--------------------|-----------------------------------|-----------------------------------|-----------------------------------|-----------------------------------|-----------------------------------|-----------------------------------|---------------------------------|--------------------------------|
| | | $\psi \leq 60^\circ$ | | $\psi \leq 72^\circ$ | | $\psi \leq 60^\circ$ | | $\psi \leq 72^\circ$ | |
| | | $N_{\gamma} P_{\gamma}(0)10^{16}$ | $N_{\gamma} P_{\gamma}(0)10^{16}$ | $N_{\gamma} P_{\gamma}(0)10^{16}$ | $N_{\gamma} P_{\gamma}(0)10^{16}$ | $N_{\gamma} P_{\gamma}(0)10^{16}$ | $N_{\gamma} P_{\gamma}(0)10^{16}$ | $N_{\gamma} J_{\gamma}10^{16}$ | $N_{\gamma} J_{\gamma}10^{16}$ |
| 1,6-2,0 | 1,73 | 237 396 | 278 | 212 822 | 276 | 370 1770 | 495 | 819 5820 | 1049 |
| 2,0-2,5 | 2,18 | 145 194 | 188 | 142 440 | 197 | 261 998 | 365 | 548 3110 | 750 |
| 2,5-3,2 | 2,77 | 78 74,1 | 98 | 85 188 | 115 | 164 447 | 210 | 327 1330 | 423 |
| 3,2-4,0 | 3,52 | 46 38,4 | 56 | 37 71,8 | 47 | 91 218 | 125 | 174 619 | 228 |
| 4,0-5,0 | 4,41 | 23 15,4 | 30 15,8 | 23 35,7 | 33 34,9 | 39 74,6 | 54 70,6 | 85 241 | 117 235 |
| 5,0-6,3 | 5,54 | 14 7,19 | 18 7,26 | 10 11,9 | 15 12,2 | 21 30,8 | 34 34,8 | 45 98,2 | 67 103 |
| 6,3-8,0 | 7,01 | 4 1,99 | 7 1,99 | 2 2,51 | 6 3,43 | 9 5,29 | 12 9,23 | 15 25,0 | 25 29,5 |
| 8,0-10,0 | 8,87 | 7 [$\bar{E}_{\gamma} = 7,77$] | 7 | 4 | 6 | 3 4,67 | 5 3,77 | 14 19,9 | 18 18,07 |
| 10,0-12,5 | 11,0 | 1 | 1 | 2 0,75 | 2 0,74 | 8 9,90 | 8 | 11 12,5 | 11 8,88 |
| 12,5-16,0 | 14,0 | | | 1 [$\bar{E}_{\gamma} = 12,4$] | 1 | 2 1,04 | 2 0,87 | 3 1,89 | 4 1,87 |
| 16,0-20,0 | 17,8 | | | | | 2 [$\bar{E}_{\gamma} = 15,8$] | 3 | 2 | 3 |

N_{γ} - is the EPC number within given energy range
 $P_{\gamma}(E_{\gamma}, 0^\circ) [g^{-1} sec^{-1} ster^{-1} rev^{-1}]$ - is the differential intensity of γ -quantum generation,
 $J_{\gamma}(E_{\gamma}) [g^{-1} sec^{-1} rev^{-1}]$ - is the global differential intensity of γ -quantum generation.

In order to find out if the cosmic ray nuclear-active component with its highest vertical intensity contributes to the detected EPC flux we examined the distribution of the generation points of EPC with zenith angles from 0° to 26° over

the chamber volume. The distribution proved to be uniform and, hence it may be asserted that all EPC are produced by muons.

Further on, all our results for the bremsstrahlung photon angular distributions and energy spectra were compared to the calculations made by Volkova (1969,1970). Transition from the spectra and angular distributions of photons to the same distributions for muons was made on the basis of these calculations. Volkova calculated the muon fluxes at sea level on several assumptions about the muon generation mechanism: decay of pions, decay of pions and some portion of kaons; decay of pions, kaons and the process of direct muon generation. The pion and kaon spectra were described by the power law with the same power exponent $\gamma = 1.65 \pm 0.05$ as for the primary nucleons over the entire energy range of interest to us. In the 30-100 Gev energy range the calculated fluxes were normalized on the basis of magnetic spectrometer measurements (Allkofer et al., 1971). In the studied (2-20) Tev energy range the muon energy spectrum proves to be of almost power form. The relation between the fluxes of muons and bremsstrahlung photons was found for such muon spectrum form including the probability of bremsstrahlung in lead:

$$\frac{D}{p_{\mu}^2} = \varepsilon(E_0, \gamma_{\mu})$$

5. Zenith angular distribution. The EPC zenith angular distribution obtained in the present work is shown in Fig.3 together with the calculated curves for the various generation mechanisms. The distribution curves for the various generation mechanisms are corrected for the muon absorption in the ground plots are corrected for the muon absorption in the ground above the installation as calculated by Gurentsov. This correction is substantial only at $\Theta \geq 80^\circ$ and is a function of muon energy, zenith angle, and ground relief.

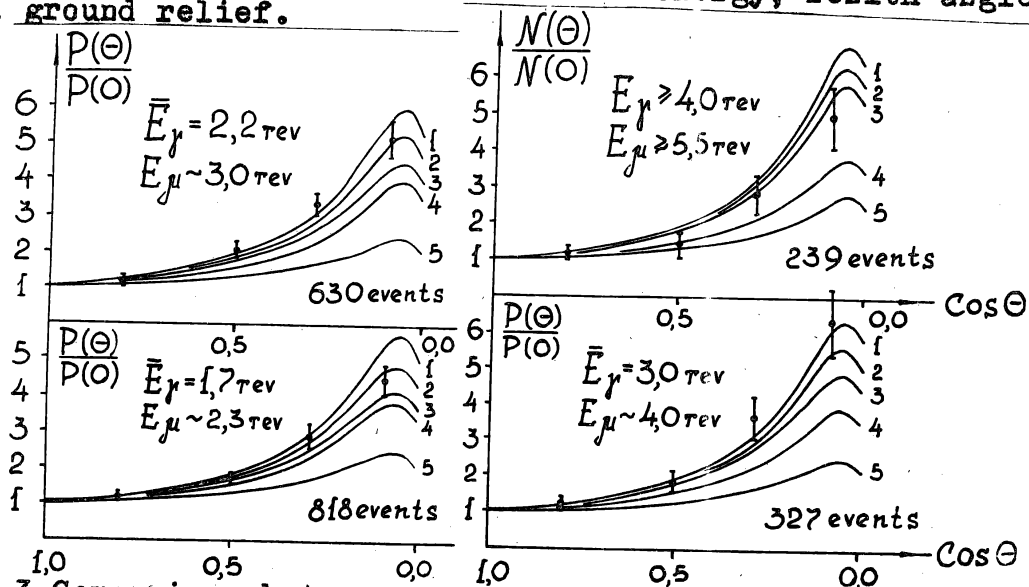


Fig.3. Comparison between the experimental and calculated zenith angular distributions for the various muon generation mechanisms: 1) π 2) $\pi+20\%K$ 3) $\pi+70\%K$ 4) $\pi+20\%K+1\%\mu$ 5) $\pi+20\%K+Utah$

Table 3 presents the ratios of the EPC number in the $0.3 \geq \cos\theta \geq 0.0$ interval to the EPC number in the $1.0 \geq \cos\theta \geq 0.6$ interval.

Table 3

| E_{μ} TeV | theory | | | | experiment |
|------------------|--------|-------------|-------------------------|---------------------------|-----------------|
| | π | $\pi+20\%K$ | $\pi+20\%K+$ $+1\%u$ | $\pi+20\%K+$ $+1\%\mu$ | |
| ≥ 2.2 | 2.82 | 2.58 | 1.38 | 2.02 | 2.72 ± 0.15 |
| ≥ 4.0 | 3.02 | 2.81 | 1.36 | 2.05 | 3.06 ± 0.38 |
| ≥ 7.0 | 3.12 | 2.95 | 1.77 | 1.80 | 2.84 ± 0.59 |

The experimental and calculated distributions were inter-compared using the χ^2 -test method. In this case the theoretical distribution was normalized to the calculated distribution for the total particle number. The results of the inter-comparison have shown that our experimental data agree with theoretical calculations made on the assumption of muon production in pion decay or in the decay of pions with a 20% admixture of kaons.

The zenith angular distributions of muons disagree with the assumption of an additional process of direct muon generation set forth in (Bergeson et al., 1967).

6. Energy spectra. The differential global EPC spectrum, $\mathcal{N}_{\gamma}(E_0)_{exp}$ obtained in the present work was compared with the calculated bremsstrahlung spectrum, $\mathcal{N}_{\gamma}(E_0)_{theory}$, of photons produced by muons in lead on the assumption that the muons are generated in the process of decay of pions and 10% of kaons. Fig.4a presents the results of this comparison. Up to ~ 6 Tev EPC energies the experimental data agree with the calculation within the experimental accuracy and then the points move aside from the curve. The number of the detected EPC with $E_0 \geq 63$ Tev is 61 instead of 100 as expected from the calculated spectrum.

For the purposes of further analysis the EPC energy spectra were examined in three zenith angle ranges: $1.0 \geq \cos\theta \geq 0.6$, $0.6 \geq \cos\theta \geq 0.3$, $0.3 \geq \cos\theta \geq 0.0$ and were similarly compared to the spectra expected from the calculations. It can be seen from Fig.4 that up to ~ 6 Tev the spectra may be, within the errors, coordinated with the assumption of a power form of the pion and kaon spectrum which repeats the primary nucleon spectrum.

The differential global spectrum of γ -quantum generation may be written as

$$\mathcal{Y}_\gamma(E) = (4.2 \pm 1.3) \cdot 10^{-13} \left(\frac{E_{\text{TeV}}}{2}\right)^{-3.55 \pm 0.12} \text{g}^{-1} \text{sec}^{-1} \text{TeV}^{-1} \quad (2 \leq E \leq 5)$$

$$\mathcal{Y}_\gamma(E) = (1.5 \pm 0.5) \cdot 10^{-14} \left(\frac{E_{\text{TeV}}}{5}\right)^{-3.8 \pm 0.3} \text{g}^{-1} \text{sec}^{-1} \text{TeV}^{-1} \quad (5 \leq E \leq 20)$$

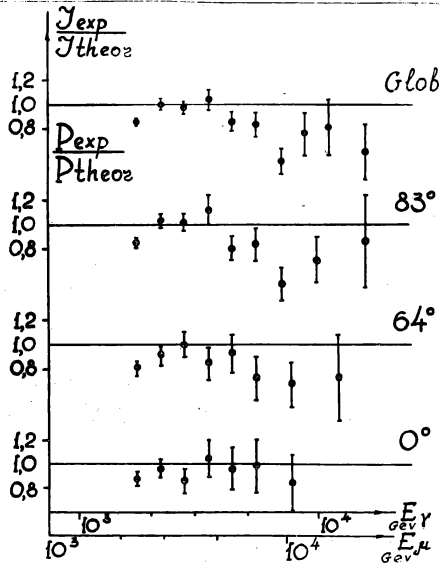


Fig.4. Ratio of the experimental to calculated bremsstrahlung photon spectra at the various angles

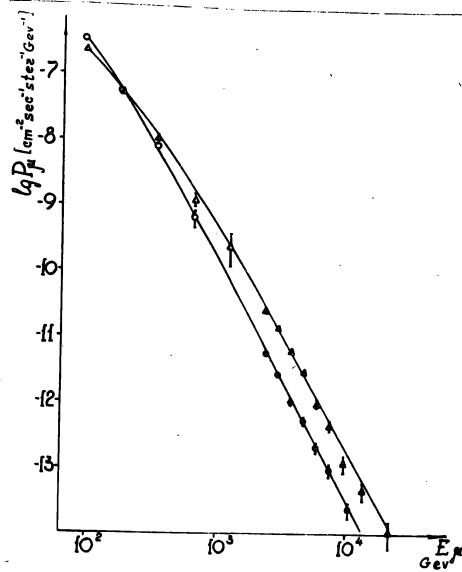


Fig. 5. Differential muon spectra:
 Allkofer $\circ \odot = 0^\circ$
 $\Delta \odot = 83^\circ$
 the present work $\bullet \odot = 0^\circ$
 $\blacktriangle \odot = 83^\circ$

The muon spectra shown in Fig.5 have been obtained including the angular distribution and absorption of muons in ground. For the sake of comparison the same figure presents the spectra from (Allkofer et al.,1971) obtained on the basis of magnetic spectrometer measurements. The solid curves have been calculated on the assumption of muon generation by pions and 10% of kaons. It can be seen from Fig.5 that the data of the present work are the direct continuation of the spectra obtained using a magnetic spectrometer in the high-energy range. The 2-7 TeV muon spectra may be written as

$$P_\mu(E, 0^\circ) = (1.04 \pm 0.3) \cdot 10^{-8} \left(\frac{E_{\text{TeV}}}{2}\right)^{-3.55 \pm 0.24} \text{cm}^{-2} \text{sec}^{-1} \text{ster}^{-1} \text{TeV}^{-1}$$

$$P_\mu(E, 83^\circ) = (5.5 \pm 1.6) \cdot 10^{-8} \left(\frac{E_{\text{TeV}}}{2}\right)^{-3.6 \pm 0.12} \text{cm}^{-2} \text{sec}^{-1} \text{ster}^{-1} \text{TeV}^{-1}$$

The global muon spectrum in all zenith angle ranges can be written as

$$J_{\mu}(E_{\mu}) = (1.7 \pm 0.5) \cdot 10^{-7} \left(\frac{E_{\text{TeV}}}{2} \right)^{-3.6 \pm 0.12} \text{ cm}^{-2} \text{ sec}^{-1} \text{ TeV}^{-1}$$

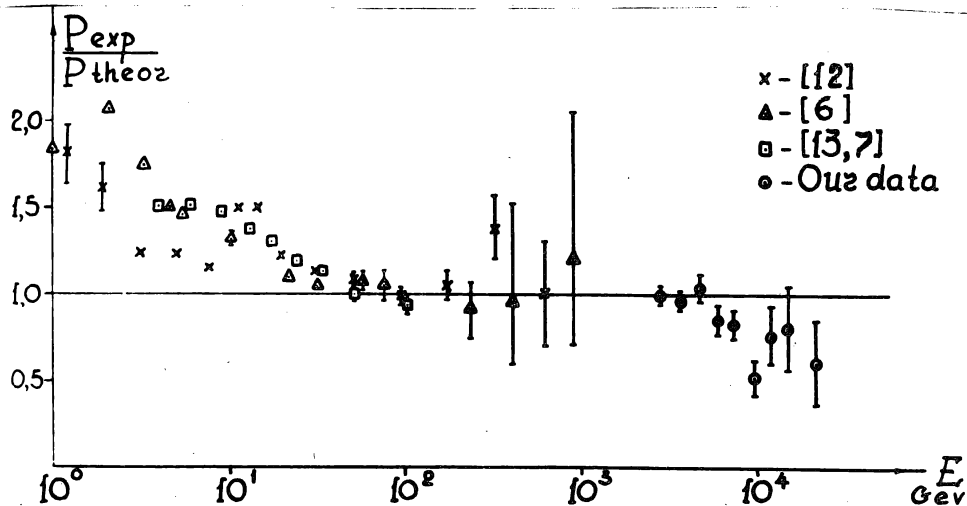


Fig.6 presents a comparison of the calculated differential energy spectra of muons generated by pions and 10% of kaons with the data obtained in the works by the various groups. As it was mentioned above the calculations were made on the assumption that the muon and kaon generation spectrum is of the same power form as the cosmic ray hadron spectrum, i.e. the scaling holds for strong interactions.

The possible 20-30% inaccuracy in determining the absolute muon intensity admits (including the data from (Allkofer et al., 1971; Appleton et al., 1971; Hayman and Wolfendale, 1962; Gardener et al., 1962; Ashton et al., 1972)) a 0.05 change in the pion and kaon spectrum slope. Thus the conclusion may be drawn that muon spectrum is in agreement with scaling in the 30-8000 Gev muon energy range, which corresponds approximately to the 10^{11} - 10^{14} hadron energies.

At energies of ~ 8 Tev the muons are somewhat scanty, which can be explained by the back statistical security with a probability of less than 1%.

The results obtained may mean that at $> 10^{14}$ ev hadron energies the scaling is violated and the number of pions with energies close to the energies of generating nucleons is decreased. The possibility of the anomalous process of high-energy muon absorption should be additionally specified.

REFERENCES

1. I.S.Alekseev, G.T.Zatzepev^s 6th Inter.Conf. on Cosmic Rays, Moscow, v.1, (1959).
2. O.C.Allkofer, K.Carstensen and W.D. Dau 12th Int. Conf. on Cosmic Rays, Hobart, v.4, 1314 (1971).
3. T.P.Amineva, K.V.Cherdyntseva 12th Int. Conf. on Cosmic Rays, Hobart, v.6 (1971).
4. T.P.Amineva, A.Ya.Varkovitskaya et al., Izv. Akad. Nauk, ser.fis. 36, 8, 1756 (1972).
5. T.P.Amineva, A.Ya.Varkovitskaya et al., Moscow Univ. Preprint (1973).
6. I.C.Appleton, M.T.Hogue, B.C.Rastin Nucl. Phys. B26, 365 (1971).
7. F.Ashton, K.Tsuji, A.W.Wolfendale Nuov.Chim. 9B, 344 (1972).
8. L.T.Baradzei et al., Lebedev Inst. Preprint 65 (1971).
9. H.E.Bergeson, J.W.Keuffel et al., Phys. Rev.Let. 19, 1487 (1967).
10. H.E.Bergeson, G.L.Bolingbroke, I.W.Keuffel et al., 12th Int.Conf. on Cosm. Rays, Hobart, v.4, 1418 (1971).
11. A.D.Erlykin et al., 12th Int. Conf. on Cosmic Rays, Hobart, v. 6, 2144 (1971).
12. O.C.Allkofer, K.Carstensen and W.D.Dau 12th Int. Conf. on Cosmic Rays, Hobart, v.4, 1314, (1971).
13. P.I.Hayman, A.W.Wolfendale Proc. Phys. Soc. 80, 710, (1962).
14. G.B.Kristiansen et al., 12th Int. Conf. on Cosmic Rays, Hobart, v.6, 2122, (1971).
15. I.Nishimura, Progr. Theor. Phys. Suppl. 32, 72 (1964).
16. L.W.Volkova Lebedev Inst. Preprint N 72 (1969).
17. L.W.Volkova Izv.Akad. Nauk SSSR, ser.fis. 34, N 9, 1982 (1970).